

000  
001  
002  
003 

# SPIKE-RL: VIDEO-LLMS MEET BAYESIAN SURPRISE

  
004  
005  
006  
007  
008  
009  
010  
011  
012  
013  
014  
015  
016  
017  
018  
019  
020  
021  
022  
023  
024  
025  
026  
027  
028  
029  
030  
031  
032  
033  
034  
035  
036  
037  
038  
039  
040  
041  
042  
043  
044  
045  
046  
047  
048  
049  
050  
051  
052  
053

**Anonymous authors**

Paper under double-blind review

## ABSTRACT

Real-world videos often show routine activities punctuated by memorable, surprising events. However, most Video-LLMs process videos by sampling frames uniformly, likely missing critical moments that define a video’s narrative. We introduce SPIKE, an inference-time framework that quantifies Bayesian Surprise as the belief update triggered by new visual evidence in the video stream, identifying moments where new visual evidence conflicts with prior beliefs. SPIKE effectively localizes surprise in videos, correlated with humans on positive (FunQA) and negative (Oops!) surprise benchmarks. SPIKE-RL further improves on SPIKE’s ability to detect surprise, leveraging GRPO to refine its belief hypotheses based on a reward signal from the video caption. SPIKE and SPIKE-RL guide query-agnostic surprise-weighted frame sampling, which allocates more frames to interesting moments in the video. With this strategy, we achieve consistent performance gains on five downstream benchmarks. By enabling Video-LLMs to track beliefs and register surprise, our work paves the way for more robust models that can revise their understanding in response to new information.<sup>1</sup>

## 1 INTRODUCTION

Humans navigate the world not as passive observers, but as active predictors of the future who infer the hidden causes behind events and update their predictions (Millidge et al., 2022). This process, formalized within the Bayesian Theory of Mind (ToM) framework (Baker et al., 2017), suggests that our brain continuously builds and updates an internal model of the world, using discrepancies between expectation and reality, or *surprise*, as the primary signal for learning and attention. This allows us to efficiently process a constant stream of sensory data, focusing our cognitive resources on moments that are novel and informative, and ignoring redundant, expected information. For instance, in the Mr. Bean video shown in Figure 1, our cognitive focus is on the moment the man unexpectedly falls, because it deviates from the established routine.

However, current Video-LLMs are fundamentally disconnected from this sequential, belief-driven process. Most models treat videos as a ‘bag of frames’, where a subset is uniformly sampled from the video (OpenAI, 2024; Bai et al., 2023; 2025; Cheng et al., 2024; Liu et al., 2023). Lacking an evolving belief about the video’s story, uniform sampling is much more likely to sample highly frequent mundane moments over rare surprising (and therefore memorable) events. This can potentially overwhelm Video-LLMs with redundant information, over pivotal moments a human observer would focus on, such as the fall in Figure 1.

To overcome this, some methods select or retrieve frames retroactively for a given textual query (Yu et al., 2025; Wang et al., 2025; 2024; Liang et al., 2024; Tang et al., 2025b). However, in dynamic, open-world settings, we often don’t know in advance what questions will be asked. What we need instead is a model that reasons *proactively*, anticipating what is surprising, and paying attention to these shifts, similar to a human observer. In this work, we study two fundamental questions to bridge this gap: (1) How can Video-LLMs proactively track and update their beliefs as new visual evidence presents itself? and (2) Can detecting semantically surprising events proactively and ahead of downstream queries improve video understanding?

To answer these, we introduce SPIKE, an inference-time framework that represents a model’s beliefs as explicit probability distributions over human-interpretable textual hypotheses, and quantifies Bayesian Surprise as the divergence between prior and posterior beliefs (Itti & Baldi, 2005), giving

<sup>1</sup>Code, data and models will be made public.



Figure 1: (a) Uniform sampling misses key moments. (b) Our surprise-based sampling focuses on high-surprise regions, strongly aligning with human laughter. (c) Our method achieves significantly better surprise localization than a zero-shot Qwen2.5-VL baseline.

us a surprise score. As shown in Figure 1(b), this surprise score pinpoints moments that contradict the model’s prior beliefs. We further improve the surprise scoring by introducing SPIKE-RL, trained using a reinforcement learning objective that teaches the model to prioritize beliefs that lead to more accurate video captions. SPIKE achieves 65.7% on FunQA (Xie et al., 2025), a surprise localization benchmark, and SPIKE-RL improves on it further, with 68.2%, significantly outperforming the zero-shot performance of Qwen2.5-VL (Figure 1(c)). Our experiments show that SPIKE-RL delivers two complementary benefits: it improves the diversity of generated belief hypotheses, and boosts surprise localization accuracy beyond what the inference-time scorer alone can achieve. Finally, we leverage this signal by replacing the standard uniform frame sampling with surprise-weighted sampling in Qwen2.5-VL and demonstrate that this leads to consistent improvements on five downstream video understanding tasks.

Our approaches allow Video-LLMs to focus on the most salient parts of the video, akin to human notions of surprise. In the future, surprise-aware Video-LLMs can be used to improve the robustness real-time applications such as streaming, surveillance, robotics, and interactive agents that need to adapt to new information on-the-fly.

## 2 BAYESIAN BELIEF TRACKING

### 2.1 SURPRISE SCORING

The architecture of SPIKE is shown in Figure 2. SPIKE quantifies Bayesian surprise by tracking how the model’s belief distribution over human-interpretable textual hypotheses shifts when a new frame is observed. Each incoming frame updates this belief distribution, and the magnitude of the change defines the surprise score. SPIKE produces surprise scores for each step, across the complete video. For simplicity, we describe this process using fixed-length videos. However, our method can be adapted to a streaming video setup by applying the same update online.

**Setup.** A video is composed of a sequence of frames  $X_{1:T}$ , where  $T$  is the length of the video. To compute surprise at a timestep  $t$ , we use three key inputs as shown in Figure 2(b): (i) the *prior window* of  $W$  frames immediately preceding the current  $t$ ,  $\mathcal{W}_t = X_{t-W:t-1}$ , (ii) a *historical summary*,  $H_t$ , a textual summary of what happened so far in the video, derived from the  $C$  frames,  $X_{t-C:t-W-1}$ , that occurred before  $\mathcal{W}_t$ ,<sup>2</sup> and (iii) the newly observed frame  $O_t = X_t$ . This setup allows the model to form beliefs based on both long-term context and recent events, and then measure surprise with respect to the new information.<sup>3</sup>

**Hypothesis Generation.** First, at timestep  $t$ , we generate a set of belief hypotheses,  $\mathcal{B}_t = \{b_{t,1}, \dots, b_{t,N}\}$ , where each hypothesis  $b$  is a textual description of what might happen next, generated by a model  $M$  by conditioning on the historical summary  $H_t$  and the prior frame window  $\mathcal{W}_t$  (Fig. 2). We use a Video-LLM as our model  $M$  and generate diverse beliefs  $\mathcal{B}_t$  using nucleus sampling (Holtzman et al., 2020).

<sup>2</sup>See Appendix B for further information on how the textual summary is obtained.

<sup>3</sup>See Appendix A.1 for the prompts for the hypothesis generation and scoring.

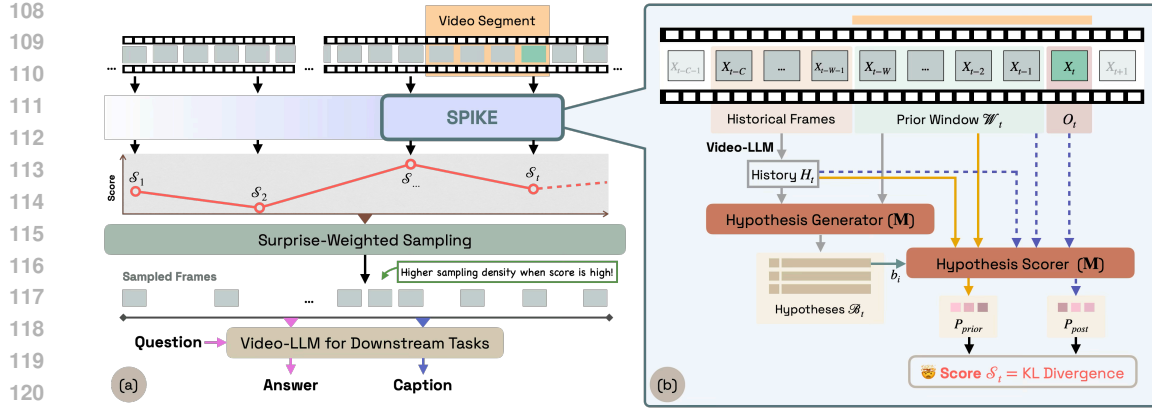


Figure 2: (a) Overall architecture: SPIKE computes surprise scores, which guide weighted frame sampling for downstream tasks. (b) SPIKE : Given history  $H_t$ , prior window  $\mathcal{W}_t$ , and observed frame  $O_t$ , the hypothesis generator produces belief set  $B_t$ . The hypothesis scorer computes  $P_{prior}$  and  $P_{post}$ , yielding surprise score  $S_t$  as KL divergence.

**Bayesian Surprise.** Next, we establish **prior** and **posterior** belief distributions over the generated beliefs  $\mathcal{B}_t$ . We define a score for each hypothesis  $b_{t,i}$  based on its plausibility, which is inversely proportional to its negative log-likelihood (NLL) as computed by the Video-LLM  $\mathbf{M}$ . This score reflects how well the hypothesis aligns with the given context.

The prior distribution  $P_{prior}$  is calculated based on the historical context ( $H_t$ ) and the recent prior window ( $\mathcal{W}_t$ ), *before* the new frame  $O_t$  is observed:

$$P_{prior}(b_{t,i} | H_t, \mathcal{W}_t) = \frac{\exp\left(-\frac{1}{\tau} \cdot \text{NLL}(b_{t,i} | H_t, \mathcal{W}_t)\right)}{\sum_{j=1}^N \exp\left(-\frac{1}{\tau} \cdot \text{NLL}(b_{t,j} | H_t, \mathcal{W}_t)\right)}, \quad (1)$$

where  $\text{NLL}(b_i | \cdot) = -\log P_{\mathbf{M}}(b_i | \cdot)$  is the negative log-likelihood of the hypothesis tokens given the context, and  $\tau$  is a temperature parameter. We apply softmax to normalize the scores into a probability distribution.

After observing the new frame  $O_t$ , we update our beliefs to form the posterior belief distribution,  $P_{post}$ , by incorporating this new visual evidence into the model's context:

$$P_{post}(b_{t,i} | H_t, \mathcal{W}_t, O_t) = \frac{\exp\left(-\frac{1}{\tau} \cdot \text{NLL}(b_{t,i} | H_t, \mathcal{W}_t, O_t)\right)}{\sum_{j=1}^N \exp\left(-\frac{1}{\tau} \cdot \text{NLL}(b_{t,j} | H_t, \mathcal{W}_t, O_t)\right)}. \quad (2)$$

Following the Bayesian formalization of surprise by Itti & Baldi (2005), we quantify our surprise score to be the information gain induced by  $O_t$ , as the Kullback–Leibler (KL) divergence between posterior and prior beliefs over hypotheses:

$$\mathcal{S}_t = D_{\text{KL}}(P_{post}(\cdot | H_t, \mathcal{W}_t, O_t) \parallel P_{prior}(\cdot | H_t, \mathcal{W}_t)) \quad (3)$$

$$= \sum_{i=1}^N P_{post}(b_{t,i}) \log \frac{P_{post}(b_{t,i})}{P_{prior}(b_{t,i})}. \quad (4)$$

Using Equation 3, at each timestep  $t$  we compute a scalar surprise score  $\mathcal{S}_t$ , as well as a belief set at  $t$  containing hypotheses and their prior and posterior probabilities,  $\mathcal{B}_t = \{(b_{t,i}, P_{prior}(b_{t,i}), P_{post}(b_{t,i}))_{i=1}^N\}_t$ .  $\mathcal{B}_t$  is human-readable and interpretable, enabling insight into *why* a video segment is surprising.

## 2.2 SURPRISE-WEIGHTED FRAME SAMPLING

Since it is computationally infeasible and impractical to process all frames of a video, Video-LLMs sample frames – by default, uniformly. Only the selected frames are then processed by the model

162 while the rest are discarded. We define frame budget,  $F$ , as the maximum number of frames that  
 163 a Video-LLM uses. Our goal is to effectively select those  $F$  frames among the video frames  $X_{1:T}$   
 164 by recognizing surprising regions of the video, which may be especially important for downstream  
 165 tasks such as captioning and question answering.

166 **Computing a Surprise-Guided Probability Distribution.** As shown in Fig 2(a), for a given  
 167 video  $X_{1:T}$ , we first uniformly sample timesteps  $t_1, \dots, t_K$ , for  $K \leq F$ . Each timestep repre-  
 168 sents the end of a video segment, on which we measure surprise; this is akin to a sliding win-  
 169 dows over the frames of the video. We use SPIKE to compute surprise scores for each seg-  
 170 ment, and obtain scores  $\mathcal{S}_1, \dots, \mathcal{S}_K \in [0, 1]$  for the corresponding timesteps  $t_1, \dots, t_K$ . We  
 171 can now modify the frame sampling to be proportional to the surprise scores. Specifically, we  
 172 compute the probability of sampling from a segment ending at  $t_i$  as the softmax over scores,  
 173  $p_i = \text{softmax}\left(\frac{s_i}{\tau_s}\right) = \frac{\exp(s_i/\tau_s)}{\sum_{j=1}^K \exp(s_j/\tau_s)}$  ( $\tau > 0$ ), and use  $p_i = 1/K$  if all  $s_i$  are equal.  $\tau_s$  is the  
 174 temperature of this softmax function.

175 **Sampling.** Given the frame budget  $F$  for the Video-LLM, we sample  $F$  frames by repeatedly  
 176 choosing a segment  $i$  with probability  $p_i$  (with replacement) and drawing a uniform timestamp  
 177 within that segment; each timestamp is mapped to a frame index via the video frame rate. Choices  
 178 are independent, so high-surprise segments can contribute multiple frames. We use  $\tau_s$  in Eq. 2.2  
 179 to control sampling: a small  $\tau_s$  concentrates the budget on surprising regions, whereas a larger  $\tau_s$   
 180 spreads the frame budget more uniformly. We set  $\tau_s = 0.7$  for our experiments.

### 182 2.3 COMPLEXITY ANALYSIS

184 Let a video contain  $T$  frames. We uniformly sample a fixed budget of  $F$  frames, so the video is  
 185 divided into  $W = T/F$  segments and one frame is drawn from each segment. For each sampled  
 186 frame we generate  $N$  text hypotheses and compute their prior and posterior likelihoods.

188 **Time Complexity.** The method requires  $F$  hypothesis-generation steps and two batched likelihood  
 189 evaluations per step. The total cost is therefore  $O(F \cdot N)$ , which is linear in the chosen frame  
 190 budget  $F$  (and therefore at most linear in  $T$  if  $F$  grows with  $T$ ). In practice, GPU parallelization  
 191 allows batching the  $N$  hypotheses at each step, amortizing the generation cost and reducing the total  
 192 complexity from  $O(F \cdot N)$  to  $O(F)$  when sufficient parallel compute is available.

194 **Relation to Inference-Time Scaling.** Our overhead is comparable to recent inference-time scaling  
 195 methods for Video-LLMs: a controllable number of extra forward passes improves where the model  
 196 allocates its fixed frame budget, without changing its architecture.

198 **Interpretability.** Because SPIKE represents beliefs as *textual hypotheses*, its Bayesian surprise  
 199 scores are interpretable: one can inspect the generated hypotheses to understand what the model  
 200 “expected” versus what the new frames revealed.

## 202 3 REINFORCEMENT LEARNING FOR BELIEF OPTIMIZATION

204 **Motivation.** The effectiveness of SPIKE relies on the model’s ability to generate belief hypothe-  
 205 ses that are accurate, diverse, and representative of the video segment shown. However, since VLMs,  
 206 are not tailored to perform belief tracking on frame windows, the model has no incentive to refine  
 207 its intermediate hypotheses. However, training SPIKE with direct supervision on this reasoning  
 208 process is intractable, as it is impractical to collect ground truth hypotheses across every segment of  
 209 a video, for a large set of videos. Instead, we leverage GRPO (Shao et al., 2024) to optimize SPIKE  
 210 using reinforcement learning. SPIKE-RL is based on the insight that a strong final caption – i.e. of  
 211 what happened in the complete video – is built upon accurate intermediate belief hypotheses – i.e.  
 212 about what is likely to happen after having watched a portion of the video.

213 Figure 3 demonstrates our approach. To train the hypothesis generator, our policy model, we com-  
 214 pute a reward signal based on the quality of the final caption. This reward signal is then propagated  
 215 backward, assigning credit to the sequence of beliefs that led to the successful outcome. In this  
 way, supervision on the final result is implicitly transformed into training feedback for the model’s

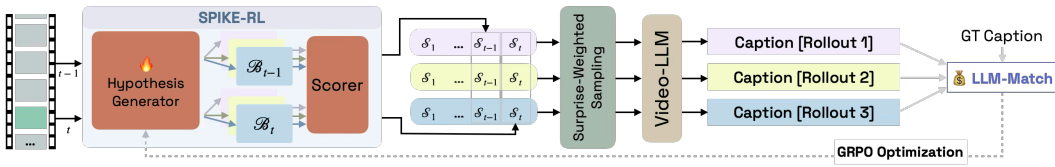


Figure 3: SPIKE-RL explores multiple hypothesis trajectories, whose surprise scores guide frame sampling. Captions from these rollouts are scored with LLM-Match, and GRPO propagates the reward to improve hypothesis generation.

internal reasoning process. Our rewards are derived from an LLM-based metric that computes the similarity between the generated caption and the ground truth caption.

**Rollout.** We design the GRPO-based training procedure by generating a group of captions, based on different *trajectories* of beliefs and frame allocations. For each video, we draw  $M$  trajectories  $\{\tau^{(r)}\}_{r=1}^M$ . Each trajectory  $\tau^{(r)}$  runs SPIKE over segments of the video. At every timestep  $t$ , it samples  $N$  textual beliefs  $\mathcal{B}_t^{(r)} = \{b_{t,1}^{(r)}, \dots, b_{t,N}^{(r)}\}$  and scores prior and posterior beliefs to obtain  $(P_{\text{prior},t}^{(r)}, P_{\text{post},t}^{(r)})$  and the surprise scores  $\mathcal{S}_t^{(r)}$ . We then use the surprise scores to inform the sampling of frames that are inputted into a Video-LLM to generate a single final video caption,  $c^{(r)}$  using our surprise-based frame allocation (§2.2). Thus each input induces a GRPO group:  $\mathcal{G} = \{(\{\mathcal{B}_t^{(r)}, \mathcal{S}_t^{(r)}\}_t^T, c^{(r)})\}_{r=1}^M$

**Reward.** At the end of a rollout, the caption  $c^{(r)}$  is scored using LLM-Match, where an LLM judge measures how similar it is to the ground truth caption, to obtain a scalar reward  $R^{(r)}$ . The prompt for the LLM judge is in Appendix A.2. We Z-score the LLM rewards within the group, and use the normalized scores as advantages in the policy objective,  $A^{(r)} = \frac{R^{(r)} - \mu_R}{\sigma_R}$ .

**Loss.** We treat the full set of hypotheses in a trajectory as a sequence-level action. Let  $p_\theta(b_{t,k} \mid H_t, \mathcal{W}_t)$  denote the policy for generating a hypothesis given the video context. We define our **belief-optimization** objective as,

$$\mathcal{L}_{\text{belief-optimization}}(\theta) = -\frac{1}{M} \sum_{r=1}^M A^{(r)} \left( \sum_t^K \sum_{k=1}^N \log p_\theta(b_{t,k}^{(r)} \mid H_t^{(r)}, \mathcal{W}_t^{(r)}) \right), \quad (5)$$

which increases the likelihood of hypotheses along high-advantage trajectories and suppresses those along low-advantage ones. Optimizing Equation 5 trains the model to generate hypotheses that reliably support strong captions, improving both the intermediate belief trajectory and the final output.

**Training.** For training SPIKE-RL, we curated a video captioning dataset of 2,000 videos with 30% *surprising* and 70% *unsurprising* videos. The goal is to expose the policy both to routine events where beliefs remain stable and to inflection points that induce belief shifts. For the unsurprising portion, we used ActivityNet Captions (Caba Heilbron et al., 2015), which predominantly includes videos depicting everyday activities. For the surprising videos, we sample from from the training set of Oops! (Epstein et al., 2020), a collection of short clips centered on unintentional human failures. We use Qwen2.5-VL-7B-Instruct as the Video-LLM model (M) and Olmo-7B-hf as the LLM-Match reward model. See App. C for the training hyperparameters.

## 4 SURPRISE LOCALIZATION

We first evaluate how well SPIKE and SPIKE-RL can identify surprising segments of a video. Hyperparameters for surprise scoring are described in App. C.

### 4.1 EXPERIMENTAL SETUP

**Benchmarks.** We evaluate surprise localization on three benchmarks: Oops! (Epstein et al., 2020), FunQA (Xie et al., 2025) and Mr. Bean (App. E). Oops! is a surprise detection task, whose test set contains 4,791 videos with precise timestamps marking the exact transition point to surprise.

270 FunQA has 424 videos with annotations for the most surprising segment in each video, given by a  
 271 start and end time. While these are established benchmarks, they only annotate a single surprising  
 272 event per video. Since our method is capable of detecting multiple surprising segments in the video,  
 273 we curate our own benchmark, Mr. Bean, using 48 clips from the live-action TV show. Mr. Bean’s  
 274 audio laughter track serves as silver-standard surprise annotations – segments of the video with  
 275 laughter are considered surprising.

276 **Metrics.** Following the protocols of Oops! and FunQA, we report Acc@0.25s and Acc@1.0s for  
 277 Oops!, and IoU for FunQA. The accuracy metrics (Acc) measure whether the predicted surprise  
 278 peak falls within 0.25 or 1.0 seconds of the ground truth peak surprise, while IoU measures the  
 279 overlap between the predicted surprising windows and the ground-truth surprising windows. For  
 280 details on the implementation of the metrics, see App. D.

281 **Baselines.** We establish a lower bound with a Random baseline that selects surprising frames at  
 282 random. We also report the zero-shot performance of our base `Qwen2.5-VL-7B-Instruct`  
 283 model, which directly scores each uniformly sampled frame on whether it is surprising or not, with-  
 284 out our proposed belief tracking mechanism (See Appendix A.3 for the prompt and setup). On  
 285 Oops!, we compare against: (i) VideoSpeed (Epstein et al., 2020), the strongest reported baseline  
 286 for this dataset; (ii) Motion Magnitude (Epstein et al., 2020), an optical-flow-based approach; and  
 287 (iii) F2C2V (Duka et al., 2022), a self-supervised method. As an upper-bound reference, we also re-  
 288 port the human consistency or agreement from the original dataset. On FunQA, we compare against  
 289 TimeChat (Ren et al., 2023), UniVTG (Lin et al., 2023), a specialized video temporal grounding  
 290 framework, and LLaVA-Next-CR, a baseline provided by the FunQA benchmark that applies the  
 291 clipping and rating (CR) technique from UniVTG to LLaVA-NeXT (Liu et al., 2024).

292

293

## 4.2 RESULTS

294

295

Table 1 shows the performance of SPIKE and SPIKE-RL on the surprise localization task. On the Oops! benchmark, our SPIKE-RL model achieves a score of 62.9% on Acc@0.25s, remarkably close to the human performance (62.1%). Notably, both SPIKE and SPIKE-RL show about a tenfold improvement over the performance of the zero-shot version of the same model (`Qwen2.5-VL-7B`). Compared to VideoSpeed, F2C2V, we observe that SPIKE and SPIKE-RL are better at accurate localization, with a 23.4% higher Acc@0.25s, and achieve similar Acc@1s scores. On the FunQA benchmark, SPIKE-RL once again demonstrates superior performance with an IoU of 68.2, surpassing both prior approaches and the zero-shot model by a substantial margin. It is worth noting that this significant boost is despite the fact that FunQA – which is composed of positive surprises related to humor and creativity – is out-of-distribution for SPIKE-RL.

305

306

307

308

309

310

Mr. Bean shows a similar trend to the other benchmarks, but the absolute Acc@0.25s is lower. This dataset is particularly challenging. In contrast to the other benchmarks, some of the surprising moments in Mr. Bean arise from subtle, fine-grained nuances in his facial expressions rather than easily noticeable unexpected events. Finally, we observe a significant 6.3% gain in IoU score with SPIKE-RL over SPIKE. Since IoU on Mr. Bean evaluates detection across multiple surprising segments, this gain highlights the ability of our scorer to capture nuanced surprises within a video.

311

312

313

Overall, the inference-time method, SPIKE, achieves superior performance across all benchmarks and generalizes to different types of surprises, while SPIKE-RL further boosts performance through reinforcement-guided refinement.

314

315

## 4.3 BELIEF SET EVALUATION

316

317

We evaluate the hypotheses generated by SPIKE and SPIKE-RL using a combination of automatic metrics and human evaluation.

318

319

**Diversity.** We are interested in whether models generate multiple conceptually-diverse hypotheses or different lexical variations of the same hypothesis. For a given video, we measure the diversity of a hypothesis set with the average inverse cosine similarity ( $1 - \cos(b_i, b_j)$ ) across all hypothesis pairs. SPIKE-RL achieves 40.3%, higher than SPIKE’s 33.5%, showing that the RL training improves diversity.

324  
325 Table 1: Performance of SPIKE and SPIKE-RL on surprise localization.  
326  
327

Method	Oops!		FunQA		Mr. Bean		
	Acc@0.25s	Acc@1s	IoU	Acc@0.25s	Acc@1s	IoU	
<i>Baselines</i>							
Random	6.8	2.6	7.5	0.6	3.5	0.9	
Motion	23.1	50.7	—	—	—	—	
Video Speed	36.6	65.3	—	—	—	—	
F2C2V	39.5	<b>69.5</b>	—	—	—	—	
TimeChat	—	—	9.6	—	—	—	
UniVTG	—	—	45.3	—	—	—	
LLaVA-NeXT-CR	—	—	62.3	—	—	—	
Qwen2.5-VL	6.6	9.6	11.6	11.2	23.2	13.8	
<b>SPIKE</b>	60.0	67.3	65.7	53.2	70.2	54.8	
<b>SPIKE-RL</b>	<b>62.9</b>	69.1	<b>68.2</b>	<b>57.4</b>	<b>78.7</b>	<b>61.1</b>	
Human	62.1	88.0	—	—	—	—	

341  
342 Table 2: Performance of Qwen2.5-VL with uniform vs. surprise-weighted and other query-free  
343 frame sampling methods. MCQ tasks are evaluated with accuracy; generative tasks with LLM-  
344 Match. Comparable open-source Video-LLMs are shown for context.

Model	Size	Sampling	BlackSwan	FunQA	ExFunTube	VideoMME-S	NextQA
VideoChat2	7B	Uniform	49.7	17.9	—	45.6	—
VideoLlama2	7B	Uniform	52.9	7.7	—	56.0	—
FunMentor	7B	Uniform	—	33.2	—	—	—
LLaVA-Video	7B	Uniform	70.4	—	—	46.6	62.7
Qwen2.5-VL	7B	Uniform	67.2	66.8	68.7	59.8	68.6
Qwen2.5-VL	7B	RGB Histogram	49.6	—	—	55.4	—
Qwen2.5-VL	7B	ECR	49.7	—	—	58.2	—
Qwen2.5-VL	7B	Katna	54.6	—	—	57.4	—
Qwen2.5-VL	7B	Optical Flow	58.6	—	—	58.1	—
Qwen2.5-VL	7B	<b>SPIKE</b>	68.8	70.3	73.2	60.8	69.8
Qwen2.5-VL	7B	SPIKE-RL	69.5	71.4	75.7	62.5	70.3
Qwen2.5-VL	32B	Uniform	69.4	72.7	71.9	69.9	72.3
Qwen2.5-VL	32B	SPIKE-RL	71.7	75.8	75.8	73.5	74.1

359  
360 **Correlation with human judgments.** We measure how well our surprise score aligns with human  
361 judgments by showing human annotators a random sample of 100 videos from Oops! along with the  
362 generated hypotheses and asking them to rank the hypotheses by dragging them onto a 0–100 scale.  
363 Each video segment is evaluated twice: first using only the prior frames ( $O_{<t}$ ), and then again after  
364 revealing the observed frame ( $O_t$ ). This setup emulates the prior and posterior probabilities in Eq. 3,  
365 from which we compute human-derived surprise scores. Comparing these to SPIKE and SPIKE-  
366 RL’s surprise scores yields a Spearman correlation of 0.84 and 0.87 respectively, indicating **very**  
367 **strong correlation** and confirming that our method effectively captures belief shifts. The template  
368 for human evaluation is provided in App. G.

369  
370 

## 5 DOWNSTREAM TASKS

371 Having shown that SPIKE and SPIKE-RL can perform surprise localization, we now explore how  
372 identifying surprising segments of the video and allocating more frames to such regions can improve  
373 a Video-LLM’s performance on downstream tasks as described in §2.2.

374  
375 

### 5.1 EXPERIMENTAL SETUP

376  
377 **Benchmarks.** We evaluate our sampling method on a diverse selection of tasks, spanning surprise  
378 explanations, question answering, and temporal reasoning. The Reporter-MCQ portion of Black-

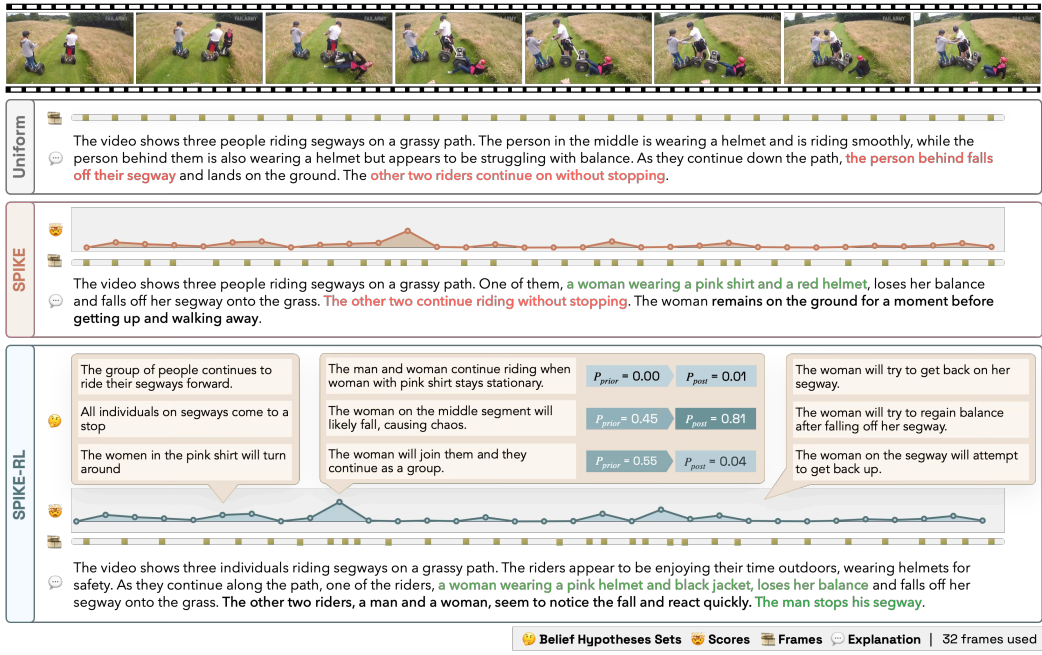


Figure 4: **Qualitative Results.** We compare Uniform, SPIKE and SPIKE-RL sampling methods. Errors in the explanation generated using uniform sampling reduce with SPIKE and are resolved with SPIKE-RL. We show belief hypotheses sets ( $\mathcal{B}_t$ ) at various timesteps, and observe how the divergence of  $P_{prior}$  and  $P_{post}$  accurately captures the surprising moment in the video.

SwanSuite (Chinchure et al., 2025) tests models’ ability to describe an unexpected event in a MCQ setup. FunQA’s Task 2 (Xie et al., 2025) and ExFunTube (Dayoon Ko, 2023) ask models to generate an explanation of why events are surprising. Moving beyond surprising videos, we test our models on two MCQ tasks – VideoMME (Fu et al., 2024), which probes general multimodal reasoning (we focus on short videos without subtitles), and NextQA (Xiao et al., 2021), which targets temporal, commonsense, and causal reasoning.

**Metrics.** Following prior work (Majumdar et al., 2024; Xie et al., 2025), we evaluate the generative tasks using LLM-Match, prompting GPT-4o to rate the similarity between model-generated and ground-truth answers. Multiple-choice tasks are evaluated using accuracy.

**Video-LLM Baselines.** We consider widely adopted open-source Video-LLMs capable of video explanation and QA, including VideoChat2 (Li et al., 2024), VideoLlama2 (Cheng et al., 2024), and LLaVA-Video (Liu et al., 2023). We also include FunMentor (Xie et al., 2025), a model specifically designed for humor understanding. Our base model is Qwen2.5-VL (7B), which we use to evaluate alternative sampling strategies under a fixed frame budget on BlackSwan and VideoMME-S. Finally, we test whether SPIKE-RL improves performance on a larger model, Qwen2.5-VL (32B).

**Query-free Frame Sampling Baselines.** To assess the effectiveness of our sampling, we benchmark against shot boundary detection methods on BlackSwan and Video-MME-S. Specifically, we tested RGB Histogram differences (V & Narayanan, 2015), Edge Change Ratio (ECR; Mann & Kaur, 2015), and motion-based detection (Wolf, 1996), which capture changes in texture, structure, motion, and similarity. In all of these approaches, salient peaks are detected via smoothed scores and frames are distributed proportionally to peak strength, ensuring that the frame budget  $F$  is met. We also include Katna,<sup>4</sup> a clustering-based method which applies K-means to frame histograms and selects the frame closest to each centroid. We use a maximum frame budget  $F$  of 64 frames for all our baselines, regardless of the sampling approach.

<sup>4</sup><https://github.com/keplerlab/katna>

432 5.2 RESULTS  
433

434 Table 2 shows the performance of SPIKE and SPIKE-RL on downstream benchmarks. On tasks  
435 with surprising videos (BlackSwan, FunQA, ExFunTube), surprise-aware sampling provides sub-  
436 stantial gains over uniform selection. Relative to uniform sampling, SPIKE improves accuracy by  
437 +1.6% on BlackSwan, +3.5% on FunQA, and +4.5% on ExFunTube. We observe that SPIKE-RL  
438 further extends performance on these tasks, with gains of +2.3% and +4.6% on BlackSwan and  
439 FunQA, and +7.0% on ExFunTube, marking our largest gains over uniform sampling. These results  
440 not only show the effectiveness of SPIKE in prioritizing surprising frames, but also credit the im-  
441 proved hypothesis quality in SPIKE-RL. On Qwen2.5-VL 32B, we see 2.3%, 3.1% and 3.9% gains  
442 respectively with SPIKE-RL, showing that our methods benefit larger models as well, extending  
443 their video understanding capability.

444 In general QA tasks (VideoMME-S, NextQA), we see moderate but consistent improvements over  
445 uniform sampling. SPIKE boosts scores by +1.0% on VideoMME-S and +1.2% on NextQA, while  
446 SPIKE-RL achieves +2.7% and +1.7% respectively on the 7B variant. The 32B variant with  
447 SPIKE-RL shows larger improvements of 3.6% and 1.8% on these tasks. These results show that  
448 surprise-aware sampling is broadly beneficial.

449 SBD strategies such as RGB Histogram, ECR, Katna, and Optical Flow consistently underperform  
450 uniform sampling. Their reliance on raw visual change makes them sensitive to camera motion and  
451 scene cuts, which rarely align with semantically important events. In contrast, our method offers  
452 principled guidance for identifying critical moments. Overall, we demonstrate that Bayesian Sur-  
453prise provides a powerful inductive signal for adaptive frame selection: SPIKE delivers immediate  
454 gains by reallocating a fixed frame budget toward more informative segments, while SPIKE-RL  
455 further improves robustness through reinforcement-guided belief optimization.

456 5.3 QUALITATIVE EXAMPLE  
457

458 Figure 4 illustrates the differences between uniform sampling, SPIKE, and SPIKE-RL. Under  
459 uniform sampling, the Video-LLM generates a caption that notes someone falling off a segway  
460 but misidentifies the person and the actions of the other riders (error highlighted in red). With  
461 the same frame budget, SPIKE and SPIKE-RL reallocate samples toward segments with high  
462 surprise scores, guided by observed belief shifts as demonstrated by the hypotheses. SPIKE correctly  
463 captures that the woman in the pink shirt and helmet loses balance and falls, though it still makes an  
464 error by stating that the other riders continue without stopping. SPIKE-RL improves on this. By  
465 more accurately localizing surprising segments – with one peak at the main fall and another smaller  
466 peak later – SPIKE-RL increases sampling density around both critical events. This leads to a more  
467 precise description of both the fall and the subsequent reactions of the other riders.

468 6 RELATED WORK  
469

470 **Belief Tracking and Updating.** Recent research in NLP has explored the idea of maintaining and  
471 updating beliefs, often with Bayesian inspired methods. Studies show that, with sufficient evidence,  
472 LLMs can approximate Bayesian updates rather than simply relying on pattern matching (Gupta  
473 et al., 2025). Closest to our work, Kim et al. (2025) explicitly maintain and re-weight hypotheses  
474 about agents’ mental states as new information becomes available, mirroring Bayesian Theory of  
475 Mind. This principle of explicit tracking also improves model robustness in complex scenarios  
476 involving multiple characters and higher-order Theory of Mind (Sclar et al., 2023). This process  
477 is closely related to the concept of defeasible reasoning, where conclusions are revised by new  
478 evidence (Rudinger et al., 2020). More broadly, the principle of Bayesian Surprise has been used as  
479 a powerful driver for exploration in other domains, such as guiding open-ended scientific discovery  
480 (Agarwal et al., 2025). We extend this idea of discovery to the domain of video understanding.

481 **Adaptive Frame Sampling Strategies for Video-LLMs.** Prior work on frame selection for Video-  
482 LLMs is primarily based on the relevance to the question. Query-conditioned methods rank frames  
483 with respect to a textual prompt to minimize redundancy while preserving task-relevant evidence.  
484 Frame-Voyager(Yu et al., 2025), Flexible Frame Selection (FFS; Buch et al., 2025) and Hu et al.  
485 (2025) learn to select informative frame sets conditioned on the query using lightweight training  
486 strategies. Adaptive Keyframe Sampling (AKS; Tang et al., 2025b) formulates selection as a

486 plug-and-play module optimizing relevance to the prompt and Guo et al. (2025) propose dynamic  
 487 keyframe search driven by visual chain-of-thought. VideoTree (Wang et al., 2025) organize a video  
 488 into a hierarchical tree and traverse it in a question adaptive manner. In contrast, our method drops  
 489 in as a replacement for the Video-LLM’s uniform sampling layer, reallocating the frame budget  
 490 towards surprising moments while remaining query-agnostic.

491 **Video Saliency and Attention.** Several works have explored video saliency and attention mecha-  
 492 nisms to focus on important frames. Hu et al. (2025) uses differential keyframe selection to choose  
 493 salient frames and differential feature merging to compress non-keyframes, focusing on query-  
 494 relevant information while reducing redundancy, thus improving long-form QA. Ma et al. (2025)  
 495 introduces Video Token Sparsification (VTS) is a CNN-based approach to reduce visual tokens for  
 496 efficient MLLM use in autonomous driving. Lee et al. (2025) introduces LLMVS, a video sum-  
 497 marization framework using LLMs to evaluate frame importance based on captions and refines it  
 498 based on global attention mechanism. Tang et al. (2025a) introduces Adaptive Keyframe Sampling  
 499 (AKS), that performs keyframe selection to maximize useful information within token limits, opti-  
 500 mizing for relevance to the prompt and coverage of the video. Azad et al. (2025) introduces HierarQ,  
 501 a hierarchical Q-Former framework that processes video frames sequentially using short and long-  
 502 term memory banks for enhanced temporal modeling and task-aware video comprehension. Koala  
 503 Tan et al. (2024) is a key frame-conditioned long Video-LLM, which uses learnable spatiotemporal  
 504 queries to adapt pretrained VLMs for longer videos. The key distinction in our work is that we  
 505 explicitly perform belief tracking, and show that our surprise is correlated with humans. Frame selec-  
 506 tion is our downstream application, but the belief tracking process could be useful for explainable  
 507 reasoning, video streaming, and training models with grounded belief trajectories in the future.

508 **Bayesian Theory of Mind and Prediction Error.** Bayesian models of social cognition frame hu-  
 509 man reasoning about others through Bayesian Theory of Mind (BToM), where observers infer latent  
 510 beliefs and goals by inverting a generative model of action Baker et al. (2009; 2017). Complement-  
 511 ing these Bayesian approaches, predictive coding theory proposes that the brain continuously  
 512 generates predictions about sensory input and uses prediction errors to update internal models Rao  
 513 & Ballard (1999); Millidge et al. (2022). Empirically Koster-Hale & Saxe (2013), extended predic-  
 514 tive coding to theory of mind, with brain activity showing reduced responses for predictable versus  
 515 unpredictable beliefs. In this integrated view Thornton et al. (2018), BToM provides the content  
 516 of the generative model (e.g., “She is thirsty”), while predictive coding describes the process of  
 517 maintaining and updating this model. SPIKE follows a similar approach of maintaining futures and  
 518 updating its belief scores.

## 520 7 CONCLUSION

521  
 522 We introduced SPIKE, a framework that lets Video-LLMs proactively register surprise. We further  
 523 showed that SPIKE-RL can refine intermediate belief generation, improving both belief diversity  
 524 and surprise localization. This enables surprise-driven frame sampling, yielding consistent gains  
 525 across downstream tasks, especially when critical information is sparse. Modeling surprise offers  
 526 a path toward understanding video narratives, adapting to violated expectations, and anticipating  
 527 events. Future work could investigate extending SPIKE to real-time streams and combining with  
 528 task-specific relevance signals.

## 532 8 REPRODUCIBILITY STATEMENT

533  
 534 We intend to make all our data, code and models open-source. SPIKE is based on an open source  
 535 Video-LLM, Qwen2.5-VL, and our training code for SPIKE-RL will be made available on GitHub.  
 536 We note that all our prompts are included in Appendix A and hyperparameters in Appendix C. For  
 537 the Mr. Bean evaluation set we create, we plan to share the video clips, along with annotations  
 538 containing their original source. We also share the instructions and template used in our human  
 539 evaluation in Appendix G.

540 REFERENCES  
541

- 542 Dhruv Agarwal, Bodhisattwa Prasad Majumder, Reece Adamson, Megha Chakravorty,  
543 Satvika Reddy Gavireddy, Aditya Parashar, Harshit Surana, Bhavana Dalvi Mishra, Andrew Mc-  
544 Callum, Ashish Sabharwal, and Peter Clark. Open-ended scientific discovery via bayesian sur-  
545prise, 2025. URL <https://arxiv.org/abs/2507.00310>.
- 546 Shehreen Azad, Vibhav Vineet, and Y. S. Rawat. Hierarq: Task-aware hierarchical q-former  
547 for enhanced video understanding. 2025 IEEE/CVF Conference on Computer Vision and Pat-  
548 tern Recognition (CVPR), pp. 8545–8556, 2025. URL <https://api.semanticscholar.org/CorpusID:276929288>.
- 549 Jinze Bai, Shuai Bai, Shusheng Yang, Shijie Wang, Sinan Tan, Peng Wang, Junyang Lin, Chang  
550 Zhou, and Jingren Zhou. Qwen-vl: A frontier large vision-language model with versatile abilities.  
551 *ArXiv preprint*, 2023.
- 552 Shuai Bai, Keqin Chen, Xuejing Liu, Jialin Wang, Wenbin Ge, Sibo Song, Kai Dang, Peng Wang,  
553 Shijie Wang, Jun Tang, Humen Zhong, Yuanzhi Zhu, Mingkun Yang, Zhaohai Li, Jianqiang Wan,  
554 Pengfei Wang, Wei Ding, Zheren Fu, Yiheng Xu, Jiabo Ye, Xi Zhang, Tianbao Xie, Zesen Cheng,  
555 Hang Zhang, Zhibo Yang, Haiyang Xu, and Junyang Lin. Qwen2.5-vl technical report, 2025.  
556 URL <https://arxiv.org/abs/2502.13923>.
- 557 Chris L. Baker, Rebecca Saxe, and Joshua B. Tenenbaum. Action understanding as inverse plan-  
558 ning. *Cognition*, 113:329–349, 2009. URL <https://api.semanticscholar.org/CorpusID:1560164>.
- 559 Chris L. Baker, Julian Jara-Ettinger, Rebecca Saxe, and Joshua B. Tenenbaum. Rational quantitative  
560 attribution of beliefs, desires and percepts in human mentalizing. *Nature Human Behaviour*, 1,  
561 2017. URL <https://api.semanticscholar.org/CorpusID:3338320>.
- 562 S. Buch, Arsha Nagrani, Anurag Arnab, and Cordelia Schmid. Flexible frame selection for ef-  
563 ficient video reasoning. 2025 IEEE/CVF Conference on Computer Vision and Pattern Recog-  
564 nition (CVPR), pp. 29071–29082, 2025. URL <https://api.semanticscholar.org/CorpusID:280654792>.
- 565 Fabian Caba Heilbron, Victor Escorcia, Bernard Ghanem, and Juan Carlos Niebles. Activitynet: A  
566 large-scale video benchmark for human activity understanding. In *Proceedings of the IEEE/CVF  
567 Conference on Computer Vision and Pattern Recognition (CVPR)*, 2015.
- 568 Zesen Cheng, Sicong Leng, Hang Zhang, Yifei Xin, Xin Li, Guanzheng Chen, Yongxin Zhu, Wenqi  
569 Zhang, Ziyang Luo, Deli Zhao, et al. Videollama 2: Advancing spatial-temporal modeling and  
570 audio understanding in video-lmms. *arXiv preprint arXiv:2406.07476*, 2024.
- 571 Aditya Chinchure, Sahithya Ravi, Raymond Ng, Vered Shwartz, Boyang Li, and Leonid Sigal. Black  
572 swan: Abductive and defeasible video reasoning in unpredictable events. In *Proceedings of the  
573 Computer Vision and Pattern Recognition Conference*, pp. 24201–24210, 2025.
- 574 Gunhee Kim Dayoon Ko, Sangho Lee. Can language models laugh at youtube short-form videos?  
575 In *The 2023 Conference on Empirical Methods in Natural Language Processing*, 2023.
- 576 Enea Duka, Anna Kukleva, and Bernt Schiele. Leveraging self-supervised training for unintentional  
577 action recognition. In *European Conference on Computer Vision Workshop SSLWIN (ECCVW)*.  
578 Springer, 2022.
- 579 Dave Epstein, Boyuan Chen, and Carl Vondrick. Oops! predicting unintentional action in video. In  
580 *The IEEE/CVF Conference on Computer Vision and Pattern Recognition (CVPR)*, June 2020.
- 581 Chaoyou Fu, Yuhang Dai, Yondong Luo, Lei Li, Shuhuai Ren, Renrui Zhang, Zihan Wang, Chenyu  
582 Zhou, Yunhang Shen, Mengdan Zhang, et al. Video-mme: The first-ever comprehensive evalua-  
583 tion benchmark of multi-modal lmms in video analysis. *arXiv preprint arXiv:2405.21075*, 2024.
- 584 Weiyu Guo, Ziyang Chen, Shaoguang Wang, Jianxiang He, Yijie Xu, Jinhui Ye, Ying Sun, and Hui  
585 Xiong. Logic-in-frames: Dynamic keyframe search via visual semantic-logical verification for  
586 long video understanding, 2025. URL <https://arxiv.org/abs/2503.13139>.

- 594 Ritwik Gupta, Rodolfo Corona, Jiaxin Ge, Eric Wang, Dan Klein, Trevor Darrell, and David M.  
 595 Chan. Enough coin flips can make LLMs act Bayesian. In Wanxiang Che, Joyce Nabende,  
 596 Ekaterina Shutova, and Mohammad Taher Pilehvar (eds.), *Proceedings of the 63rd Annual Meet-  
 597 ing of the Association for Computational Linguistics (Volume 1: Long Papers)*, pp. 7634–7655,  
 598 Vienna, Austria, July 2025. Association for Computational Linguistics. ISBN 979-8-89176-  
 599 251-0. doi: 10.18653/v1/2025.acl-long.377. URL <https://aclanthology.org/2025.acl-long.377/>.  
 600
- 601 Ari Holtzman, Jan Buys, Li Du, Maxwell Forbes, and Yejin Choi. The curious case of neural text  
 602 degeneration. In *International Conference on Learning Representations*, 2020. URL <https://openreview.net/forum?id=rygGQyrFvH>.  
 603
- 604 Kai Hu, Feng Gao, Xiaohan Nie, Peng Zhou, Son Tran, Tal Neiman, Lingyun Wang, Mubarak  
 605 Shah, Raffay Hamid, Bing Yin, and Trishul M. Chilimbi. M-ilm based video frame selection  
 606 for efficient video understanding. *2025 IEEE/CVF Conference on Computer Vision and Pattern  
 607 Recognition (CVPR)*, pp. 13702–13712, 2025. URL <https://api.semanticscholar.org/CorpusID:276647361>.  
 608
- 609 Laurent Itti and Pierre Baldi. Bayesian surprise attracts human attention. In Y. Weiss,  
 610 B. Schölkopf, and J. Platt (eds.), *Advances in Neural Information Processing Systems*, volume 18.  
 611 MIT Press, 2005. URL [https://proceedings.neurips.cc/paper\\_files/paper/2005/file/0172d289da48c48de8c5ebf3de9f7ee1-Paper.pdf](https://proceedings.neurips.cc/paper_files/paper/2005/file/0172d289da48c48de8c5ebf3de9f7ee1-Paper.pdf).  
 612
- 613 Hyunwoo Kim, Melanie Sclar, Tan Zhi-Xuan, Lance Ying, Sydney Levine, Yang Liu, Joshua B.  
 614 Tenenbaum, and Yejin Choi. Hypothesis-driven theory-of-mind reasoning for large language  
 615 models. In *Second Conference on Language Modeling*, 2025. URL <https://openreview.net/forum?id=yGQqTuSJPk>.  
 616
- 617 Jorie Koster-Hale and Rebecca Saxe. Theory of mind: A neural prediction problem.  
 618 *Neuron*, 79(5):836–848, 2013. ISSN 0896-6273. doi: <https://doi.org/10.1016/j.neuron.2013.08.020>. URL <https://www.sciencedirect.com/science/article/pii/S089662731300754X>.  
 619
- 620 Min Jung Lee, Dayoung Gong, and Minsu Cho. Video summarization with large language models.  
 621 *2025 IEEE/CVF Conference on Computer Vision and Pattern Recognition (CVPR)*, pp. 18981–  
 622 18991, 2025. URL <https://api.semanticscholar.org/CorpusID:277787286>.  
 623
- 624 Kunchang Li, Yali Wang, Yinan He, Yizhuo Li, Yi Wang, Yi Liu, Zun Wang, Jilan Xu, Guo Chen,  
 625 Ping Luo, et al. Mvbench: A comprehensive multi-modal video understanding benchmark. In  
 626 *Proceedings of the IEEE/CVF Conference on Computer Vision and Pattern Recognition*, pp.  
 627 22195–22206, 2024.
- 628 Hao Liang, Jiapeng Li, Tianyi Bai, Xijie Huang, Linzhuang Sun, Zhengren Wang, Conghui He,  
 629 Bin Cui, Chong Chen, and Wentao Zhang. Keyvideollm: Towards large-scale video keyframe  
 630 selection. *ArXiv*, abs/2407.03104, 2024. URL <https://api.semanticscholar.org/CorpusID:270924158>.  
 631
- 632 Kevin Qinghong Lin, Pengchuan Zhang, Joya Chen, Shraman Pramanick, Difei Gao, Alex Jin-  
 633 peng Wang, Rui Yan, and Mike Zheng Shou. Univtg: Towards unified video-language temporal  
 634 grounding, 2023.
- 635 Haotian Liu, Chunyuan Li, Yuheng Li, and Yong Jae Lee. Improved baselines with visual instruction  
 636 tuning, 2023.
- 637 Haotian Liu, Chunyuan Li, Yuheng Li, Bo Li, Yuanhan Zhang, Sheng Shen, and Yong Jae Lee.  
 638 Llava-next: Improved reasoning, ocr, and world knowledge, January 2024. URL <https://llava-vl.github.io/blog/2024-01-30-llava-next/>.  
 639
- 640 Yunsheng Ma, Amr Abdelraouf, Rohit Gupta, Ahmadreza Moradipari, Ziran Wang, and Kyungtae  
 641 Han. Video token sparsification for efficient multimodal llms in driving visual question answering.  
 642 In *2025 IEEE Intelligent Vehicles Symposium (IV)*, pp. 2235–2242, 2025. doi: 10.1109/IV64158.  
 643 2025.11097438.

- 648 Arjun Majumdar, Anurag Ajay, Xiaohan Zhang, Pranav Putta, Sriram Yenamandra, Mikael Henaff,  
 649 Sneha Silwal, Paul Mcvay, Oleksandr MakSYMets, Sergio Arnaud, et al. Openeqa: Embodied  
 650 question answering in the era of foundation models. In *Proceedings of the IEEE/CVF conference*  
 651 *on computer vision and pattern recognition*, pp. 16488–16498, 2024.
- 652 Jaspreet Kaur Mann and Navjot Kaur. Key frame extraction from a video using edge change ratio.  
 653 2015. URL <https://api.semanticscholar.org/CorpusID:52062936>.
- 654 Beren Millidge, Anil Seth, and Christopher L Buckley. Predictive coding: a theoretical and experi-  
 655 mental review, 2022. URL <https://arxiv.org/abs/2107.12979>.
- 656 Taisei Omine, Kenta Akita, and Reiji Tsuruno. Robust laughter segmentation with automatic diverse  
 657 data synthesis. In *Interspeech 2024*, pp. 4748–4752, 2024. doi: 10.21437/Interspeech.2024-1644.
- 658 OpenAI. GPT-4o system card, 2024.
- 659 Alec Radford, Jong Wook Kim, Tao Xu, Greg Brockman, Christine McLeavey, and Ilya Sutskever.  
 660 Robust speech recognition via large-scale weak supervision. In *International conference on ma-  
 661 chine learning*, pp. 28492–28518. PMLR, 2023.
- 662 Rajesh P. N. Rao and Dana H. Ballard. Predictive coding in the visual cortex: a functional interpre-  
 663 tation of some extra-classical receptive-field effects. *Nature Neuroscience*, 2:79–87, 1999. URL  
 664 <https://api.semanticscholar.org/CorpusID:221608503>.
- 665 Shuhuai Ren, Linli Yao, Shicheng Li, Xu Sun, and Lu Hou. Timechat: A time-sensitive mul-  
 666 timodal large language model for long video understanding. 2024 IEEE/CVF Conference on  
 667 *Computer Vision and Pattern Recognition (CVPR)*, pp. 14313–14323, 2023. URL <https://api.semanticscholar.org/CorpusID:265608767>.
- 668 Rachel Rudinger, Vered Shwartz, Jena D. Hwang, Chandra Bhagavatula, Maxwell Forbes, Ro-  
 669 nan Le Bras, Noah A. Smith, and Yejin Choi. Thinking like a skeptic: Defeasible inference  
 670 in natural language. In Trevor Cohn, Yulan He, and Yang Liu (eds.), *Findings of the Associa-  
 671 tion for Computational Linguistics: EMNLP 2020*, pp. 4661–4675, Online, November 2020.  
 672 Association for Computational Linguistics. doi: 10.18653/v1/2020.findings-emnlp.418. URL  
 673 <https://aclanthology.org/2020.findings-emnlp.418/>.
- 674 Melanie Sclar, Sachin Kumar, Peter West, Alane Suhr, Yejin Choi, and Yulia Tsvetkov. Minding  
 675 language models’ (lack of) theory of mind: A plug-and-play multi-character belief tracker. In  
 676 Anna Rogers, Jordan Boyd-Graber, and Naoaki Okazaki (eds.), *Proceedings of the 61st Annual  
 677 Meeting of the Association for Computational Linguistics (Volume 1: Long Papers)*, pp. 13960–  
 678 13980, Toronto, Canada, July 2023. Association for Computational Linguistics. doi: 10.18653/  
 679 v1/2023.acl-long.780. URL <https://aclanthology.org/2023.acl-long.780/>.
- 680 Zhihong Shao, Peiyi Wang, Qihao Zhu, Runxin Xu, Junxiao Song, Xiao Bi, Haowei Zhang,  
 681 Mingchuan Zhang, Y. K. Li, Y. Wu, and Daya Guo. Deepseekmath: Pushing the limits of mathe-  
 682 matical reasoning in open language models, 2024. URL <https://arxiv.org/abs/2402.03300>.
- 683 Reuben Tan, Ximeng Sun, Ping Hu, Jui hsien Wang, Hanieh Deilamsalehy, Bryan A. Plummer,  
 684 Bryan Russell, and Kate Saenko. Koala: Key frame-conditioned long video-llm. 2024 IEEE/CVF  
 685 Conference on Computer Vision and Pattern Recognition (CVPR), pp. 13581–13591, 2024. URL  
 686 <http://ieeexplore.ieee.org/stamp/stamp.jsp?tp=&arnumber=10658423>.
- 687 Xi Tang, Jihao Qiu, Lingxi Xie, Yunjie Tian, Jianbin Jiao, and Qixiang Ye. Adaptive keyframe sam-  
 688 pling for long video understanding. 2025 IEEE/CVF Conference on Computer Vision and Pattern  
 689 Recognition (CVPR), pp. 29118–29128, 2025a. URL <https://api.semanticscholar.org/CorpusID:276725474>.
- 690 Xi Tang, Jihao Qiu, Lingxi Xie, Yunjie Tian, Jianbin Jiao, and Qixiang Ye. Adaptive keyframe  
 691 sampling for long video understanding. *arXiv preprint arXiv:2502.21271*, 2025b.
- 692 Mark A. Thornton, Miriam E. Weaverdyck, and Diana I. Tamir. The social brain automatically  
 693 predicts others’ future mental states. *The Journal of Neuroscience*, 39:140 – 148, 2018. URL  
 694 <https://api.semanticscholar.org/CorpusID:53263667>.

- 702 Sheena C V and N.K. Narayanan. Key-frame extraction by analysis of histograms of video frames  
 703 using statistical methods. *Procedia Computer Science*, 70:36–40, 2015. URL <https://api.semanticscholar.org/CorpusID:61942704>.  
 704
- 705 Haibo Wang, Chenghang Lai, Yixuan Sun, and Weifeng Ge. Weakly supervised gaussian con-  
 706 trastive grounding with large multimodal models for video question answering. *Proceedings*  
 707 *of the 32nd ACM International Conference on Multimedia*, 2024. URL <https://api.semanticscholar.org/CorpusID:267060847>.  
 708
- 710 Ziyang Wang, Shoubin Yu, Elias Stengel-Eskin, Jaehong Yoon, Feng Cheng, Gedas Bertasius, and  
 711 Mohit Bansal. Videotree: Adaptive tree-based video representation for llm reasoning on long  
 712 videos. In *Proceedings of the Computer Vision and Pattern Recognition Conference (CVPR)*, pp.  
 713 3272–3283, June 2025.
- 714 Wayne H. Wolf. Key frame selection by motion analysis. *1996 IEEE International Conference on*  
 715 *Acoustics, Speech, and Signal Processing Conference Proceedings*, 2:1228–1231 vol. 2, 1996.  
 716 URL <https://api.semanticscholar.org/CorpusID:7256933>.  
 717
- 718 Junbin Xiao, Xindi Shang, Angela Yao, and Tat-Seng Chua. Next-qa: Next phase of question-  
 719 answering to explaining temporal actions. In *Proceedings of the IEEE/CVF Conference on Com-*  
 720 *puter Vision and Pattern Recognition (CVPR)*, pp. 9777–9786, June 2021.
- 721 Binzhu Xie, Sicheng Zhang, Zitang Zhou, Bo Li, Yuanhan Zhang, Jack Hessel, Jingkang Yang,  
 722 and Ziwei Liu. Funqa: Towards surprising video comprehension. In *European Conference on*  
 723 *Computer Vision*, pp. 39–57. Springer, 2025.
- 724 Sicheng Yu, CHENGKAI JIN, Huanyu Wang, Zhenghao Chen, Sheng Jin, ZHONGRONG ZUO,  
 725 XU XIAOLEI, Zhenbang Sun, Bingni Zhang, Jiawei Wu, Hao Zhang, and Qianru Sun. Frame-  
 726 voyager: Learning to query frames for video large language models. In *The Thirteenth Interna-*  
 727 *tional Conference on Learning Representations*, 2025. URL <https://openreview.net/forum?id=LNL7zKvm7e>.  
 728
- 729
- 730
- 731
- 732
- 733
- 734
- 735
- 736
- 737
- 738
- 739
- 740
- 741
- 742
- 743
- 744
- 745
- 746
- 747
- 748
- 749
- 750
- 751
- 752
- 753
- 754
- 755

756 **A PROMPTS**  
757758 **A.1 HYPOTHESIS PROMPTS**  
759760 **Generation.** We prompt the model with a memory of prior events and recent frames, asking for a  
761 concise next-frame prediction (8–10 words):  
762763 Given a textual summary of the video so far and the most recent *prior window of frames*, predict  
764 what will most likely happen in the next frame.  
765**Context so far:** memory\_text**Prior window (video inputs):** A sequence of images corresponding to the last  $W$  frames.**Output format:** Hypothesis: 8–10 words769 **Prior.** We use the following prompt to score each hypothesis.  
770771 **Context so far:** memory\_text772 **Prior window (video inputs):** A sequence of images corresponding to the last  $W$  frames.773 **Current frame:** The observed frame immediately following the prior window.

774 Here is what will happen next: [hypothesis statement]

775  
776 **Posterior.** We use the following prompt to score each hypothesis and compute the probability of yes  
777 as the posterior likelihood of that hypothesis.  
778779 You are given a textual summary of the video so far, a *prior window* of frames, and the *current*  
780 *frame* that follows. Your task is to evaluate whether each hypothesis generated from the prior  
781 context still holds in the current frame.782 **Context so far:** memory\_text783 **Prior window (video inputs):** A sequence of images corresponding to the last  $W$  frames.784 **Current frame:** The observed frame immediately following the prior window.785 **Hypothesis:** [hypothesis statement]786 Question: Is this hypothesis true in the *current frame*? Answer with a single word: yes or no.787 **A.2 LLM REWARD PROMPT**  
788789 Rate how closely the content of the prediction matches the content of the reference description  
790 in terms of meaning and how well it captures important details regarding events in the video.  
791 Ignore the difference in length. Score 0.0-1.0 where:792 0.0-0.3: Poor match (key details in the reference are missing in the prediction) 0.4-0.6: Mod-  
793 erate match (a few key details in the reference are captured in the prediction) 0.7-0.9: Good  
794 match (most key details are present in the prediction) 1.0: Perfect match (all key details in the  
795 reference are accurately captured in the prediction) Output only the numerical score (e.g., 0.75).796 **Reference:** gt797 **Response:** response

798 Score:

801 **A.3 ZERO-SHOT SCORER PROMPT**  
802803 You are analyzing video frames for surprisingness. For each frame, assign a label of 1 if it is  
804 surprising and 0 if it is not.  
805

806 1: surprising content

807 0: expected content

808  
809 **Video frames:** Original Video Frames

810 B HISTORICAL SUMMARY  
811

812 In our implementation, the memory of what happened since the beginning of the video i.e the His-  
813 torical summary, is maintained as a rolling textual summary that updates with each newly observed  
814 frame. Before use, the memory is compressed using the BART-Large-CNN summarization model  
815 whenever it exceeds approximately 200 word. For each step, the model receives the condensed  
816 memory, a short window of prior frames, and the most recent observed frame, and generates a cap-  
817 tion describing the new event. This caption is appended to the memory, yielding a continuously  
818 updated narrative of “what has happened so far”, which is then used for hypothesis generation and  
819 surprise computation.

820  
821 C HYPERPARAMETERS  
822823 C.1 TRAINING  
824

825 We train using 4 H100s on a single node with DeepSpeed ZeRO-3 offload. All runs use Qwen2.5-  
826 VL-7B-Instruct as the backbone, with FlashAttention-2, bfloat16 precision, and PEFT enabled.

827  
828 Table 3: Key hyperparameters for GRPO training.  
829

830 Hyperparameter	831 Value
831 Learning rate	$1 \times 10^{-6}$
832 GRPO $\beta$	0.1
833 Number of GRPO Rollouts	3
834 Number of Hypotheses per window	3
835 Max prompt length	8192 tokens
836 Training samples	2000
837 Epochs	1
838 Per-device batch size	1
839 Effective global batch size	4
840 Random seed	42

841  
842 C.2 INFERENCE  
843

844 For both SPIKE and SPIKE-RL, we maintain a hypothesis set  $N = 3$  per time step. We use a  
845 prior window of  $W = 4$  frames, and the frames for surprise scoring are allocated in proportion to  
846 the video duration,  $F = f(\text{duration})$ . Videos up to a minute are assigned a base budget of 8 frames.  
847 For longer videos, the budget continues to double with each additional minute.

848  
849 D SURPRISE LOCALIZATION METRICS  
850

851 **Accuracy@ $\delta$ .** Let  $\hat{t}$  be the predicted time (in seconds) obtained by converting the frame with the  
852 highest surprise score to time, and let  $t^*$  be the ground-truth transition time. We use the transition  
853 time provided in Oops! directly. For FunQA and Mr.Bean, center of the most surprising window is  
854 used as transition time. The instance-level score is

$$855 \text{Accuracy}@{\delta} = \mathbb{1}[|\hat{t} - t^*| \leq \delta],$$

856 and the reported metric is the mean of this indicator over the evaluation videos. Typical choices  
857 include  $\delta \in \{0.25, 1.0\}$  seconds.

858 **IoU.** Let  $\mathcal{W}_{\text{pred}} = \{[a, b] : s(t) > \tau \text{ for } t \in [a, b]\}$  be the predicted surprising windows and  $\mathcal{W}_{\text{gt}}$  be  
859 the given set of ground truth surprising windows. The Temporal IoU is:

$$860 \text{Temporal IoU} = \frac{\text{intersection coverage}}{\text{union coverage}} = \frac{|\bigcup \mathcal{W}_{\text{pred}} \cap \bigcup \mathcal{W}_{\text{gt}}|}{|\bigcup \mathcal{W}_{\text{pred}} \cup \bigcup \mathcal{W}_{\text{gt}}|}$$

864 where  $|\cdot|$  denotes temporal coverage (total duration). We define predicted surprising windows as a set  
 865 of maximal contiguous intervals where the surprise score exceeds a threshold  $\tau = 0.8 \times \max_t s(t)$   
 866 for that video.

## 868 E MR. BEAN

870 We collect 48 videos from Mr. Bean compilation videos on YouTube. Specifically, we follow this  
 871 process:

- 873 1. Each clip is divided into its scenes using a scene detector model, PySceneDetect, using its  
 874 ContentDetector<sup>5</sup>, with a threshold of 30.
- 875 2. Scenes shorter than 12 seconds and longer than 60 seconds are filtered out, to reduce incor-  
 876 rect scene cuts or have videos that are too short for our analysis.
- 877 3. We extract the audio from these scenes, and use a laughter segmentation model from Omine  
 878 et al. (2024) to identify where laughter is present. We filter scenes to obtain only those that  
 879 have 1 to 3 laughter segments.
- 880 4. Because we rely on laughter tracks as our silver-standard surprise annotation, we transcribe  
 881 the audio in these clips. We use OpenAI’s Whisper (Radford et al., 2023), with the *turbo*  
 882 model. If a clip has too many words in its transcription ( $> 8$ ), it is discarded. Through  
 883 empirical observation, we found that laughter occurs in small peaks. We ensure that at  
 884 least one such loud peak ( $> -28dB$ ) of at least 1 second occurs.
- 885 5. As a final step, we manually filter through the video set to discard scenes which contain ad-  
 886 dditional noises (e.g. bells) or scenes that are not semantically meaningful (e.g. the opening  
 887 credits) that may have passed the other filters. This leaves us with 48 video clips.

889 The full list of clips, a link to their original source, along with video scenes which we use, will be  
 890 provided with the code and data release.

## 892 F JSD

894 For bounded and symmetric reporting, we convert KL to the Jensen–Shannon divergence (JSD),  
 895 where,

$$897 \mathcal{S}_t = \text{JSD}(P_{\text{post}}, P_{\text{prior}}) = \frac{1}{2} D_{\text{KL}}(P_{\text{post}}\|M) + \frac{1}{2} D_{\text{KL}}(P_{\text{prior}}\|M), \quad (6)$$

899 where  $M = \frac{1}{2}(P_{\text{post}} + P_{\text{prior}})$ , which maps naturally to  $[0, 1]$  after  $\log_2$  normalization.

## 901 G HUMAN EVALUATION TEMPLATE

903 Fig A1 and Fig A2 show the template and instructions used for human evaluation.

905  
 906  
 907  
 908  
 909  
 910  
 911  
 912  
 913  
 914  
 915  
 916  
 917

---

<sup>5</sup><https://www.scenedetect.com/docs/0.6.1/api/detectors.html>

918  
919  
920  
921  
922  
923  
924  
925  
926  
927  
928  
929  
930  
931  
932  
933  
934  
935  
936  
937  
938  
939



< Previous Frame 8 of 8 Next >

940  
941  
942  
943 Drag each hypothesis onto the scale (0–100): top is most likely (100),  
944 bottom is impossible (0).  
945  
946  
947  
948  
949  
950  
951  
952  
953  
954  
955  
956  
957  
958  
959  
960  
961  
962  
963  
964  
965

70–100: Most likely

50–70: Definitely plausible

30–50: Likely

10–30: Unlikely

0–10: Terrible / impossible

Hyp 1: the paddleboard and its occupant will sink further under the water's surface as they drift away.

Hyp 2: the paddleboard will continue to float on its side with the person now submerged in the water below it

Hyp 3: the person may try to right the paddleboard or float in the water.

**Hypothesis 1:**  
the paddleboard and its occupant will sink further under the water's surface as they drift away.  
Score: -  
Optional note (why you placed it there)

**Hypothesis 2:**  
the paddleboard will continue to float on its side with the person now submerged in the water below it  
Score: -  
Optional note (why you placed it there)

**Hypothesis 3:**  
the person may try to right the paddleboard or float in the water.  
Score: -  
Optional note (why you placed it there)

966 Figure A1: We ask human evaluators to score the hypotheses by dragging and dropping them into  
967 likelihood bands between 0 – 100. This is repeated twice – by scoring the hypothesis with and  
968 without the observed new frame.  
969  
970  
971

972  
973  
974  
975  
976  
977  
978  
979  
980  
981  
982  
983  
984  
985  
986  
987  
988  
989  
990

## 991 Task Instructions

992

993 **Goal:** You will be shown the frames of a video one after another. For each frame, score each hypothesis based  
994 only on what frames have been seen so far.

- 995 • Use the slider or Next/Previous to move between frames.
- 996 • Only use visual evidence from frames you have seen so far (from the start up to the current frame).
- 997 • For each hypothesis shown at the current frame, assign a **likelihood score (0–100)** by dragging Hyp1,  
998 Hyp2 and Hyp3 boxes into the colored band shown on the left:
  - 999 ◦ **0–10 – Terrible/Impossible:** Contradicted by what you have seen so far.
  - 1000 ◦ **10–30 – Unlikely:** Little support; seems implausible given the evidence so far.
  - 1001 ◦ **30–50 – Likely:** Supported by several cues; plausible given the evidence so far.
  - 1002 ◦ **50–70 – Definitely plausible to 70–100 – Most likely:** Strongly supported.
- 1003 • Optional: add a short note explaining why you chose the score.

1004 .....

1005 Figure A2: Instructions shown to human evaluators.

1006  
1007  
1008  
1009  
1010  
1011  
1012  
1013  
1014  
1015  
1016  
1017  
1018  
1019  
1020  
1021  
1022  
1023  
1024  
1025